Denitrification by bradyrhizobia under feast and famine and the role of the bc1 complex in securing electrons for N_2O reduction

Yuan Gao, Magnus Øverlie Arntzen, Morten Kjos, Lars R. Bakken and Åsa Frostegård

Faculty of Chemistry, Biotechnology and Food Sciences, Norwegian University of Life Sciences, N-1432 Ås, Norway

Abstract

Rhizobia living as microsymbionts inside nodules have stable access to carbon substrates, but also have to survive as free-living bacteria in soil where they are starved for carbon and energy most of the time. Many rhizobia can denitrify, thus switch to anaerobic respiration under low O_2 tension using N-oxides as electron acceptors. The cellular machinery regulating this transition is relatively well-known from studies under optimal laboratory conditions, while little is known about this regulation in starved organisms. It is, for example, not known if the strong preference for N_2O- over NO_3^--reduction in bradyrhizobia is retained under carbon limitation. Here we show that starved cultures of a *Bradyrhizobium* strain with respiration rates 1-18% of well-fed cultures, reduced all available N_2O before touching provided NO_3^-. Proteomics showed similar abundance of Nap (periplasmic NO_3^- reductase) and NosZ (N_2O reductase), suggesting that competition between electron pathways to Nap and NosZ favoured N_2O reduction also in starved cells, similar to well-fed cultures. This contrasts the general notion that NosZ activity diminishes under carbon limitation. The results suggest that bradyrhizobia carrying NosZ can act as strong sinks for N_2O under natural conditions and that this criterion should be considered in the development of biofertilizers.

24

25 **Importance**

26 Legume cropped farmlands account for substantial N_2O emissions globally. Legumes are
27 commonly inoculated with N_2-fixing bacteria, rhizobia, to improve crop yields. Rhizobia
28 belonging to *Bradyrhizobium*, the micro-symbionts of several economically important legumes,
29 are generally capable of denitrification but many lack genes encoding N_2O reductase and will be
30 N_2O sources. Bradyrhizobia with complete denitrification will instead act as sinks since N_2O-
31 reduction efficiently competes for electrons over nitrate reduction in these organisms. This
32 phenomenon has only been demonstrated under optimal conditions and it is not known how
33 carbon substrate limitation, which is the common situation in most soils, affects the
34 denitrification phenotype. Here we demonstrate that bradyrhizobia retain their strong
35 preference for N_2O under carbon starvation. The findings add basic knowledge about
36 mechanisms controlling denitrification and support the potential for developing novel methods
37 for greenhouse gas mitigation based on legume inoculants with the dual capacity to optimize
38 N_2-fixation and minimize N_2O emission.

39

40 **Introduction**

41 Bacteria in most natural and engineered environments are faced with fluctuating availability of
42 nutrients and need to adapt to a "feast and famine" lifestyle. While many soil types are rich in
43 total organic carbon, the concentration of bioavailable carbon substrate is low, particularly in
44 non-rhizosphere soil where lack of substrate is a major factor limiting the growth of
45 heterotrophic bacteria (1). It is likely that bacteria in soil are starved most of the time (2) and

46 only experience infrequent episodes of ample provision of carbon substrate, for example as
47 exudates from a root or organic material released during decay of dead (micro)organisms.
48 Bacteria have developed several strategies to survive extended periods of starvation, such as
49 the development of high-affinity uptake systems to scavenge alternative carbon sources from
50 the surroundings, as well as changes in cell morphology, condensation of the nucleoid and
51 decreased protein synthesis to adapt to a low metabolic activity (3). Many bacteria produce
52 carbon-rich storage materials such as PHA (poly-3-hydroxyalkanoates) and glycogen during
53 periods of substrate availability, which can be utilized to sustain a minimum of metabolic
54 activity when deprived of carbon and energy (4,5).

55 Several of the microbially mediated processes in the global nitrogen cycle are closely linked
56 to the carbon (C) metabolism of the organisms. One example is denitrification, which is the
57 reduction of NO_3^- to N_2 through anaerobic respiration where the N-oxides are used as terminal
58 electron acceptors when O_2 becomes scarce. This process can be performed by a diverse range
59 of heterotrophic bacteria, archaea and fungi, which use various forms of organic compounds as
60 electron donors to obtain energy (6) or, in some cases, H_2 (7). The last step of denitrification is
61 the reduction of N_2O, a strong climate gas, to harmless N_2, catalyzed by the N_2O reductase
62 (Nos) (8,9). It is found in a diverse range of prokaryotic organisms but has not been reported in
63 eukaryotes. Some denitrifying prokaryotes can perform all steps of denitrification, others only
64 some, and lack of the last step is common due to absence of the *nosZ* gene coding for NosZ , or
65 lack of other essential gene(s) in the *nos* operon (10,11), but the amounts of N_2O released from
66 denitrification in relation to N_2 (the N_2O/N_2 product ratio) is also influenced by transcriptional
67 and post-transcriptional control mechanisms and by various environmental factors (6,12-19).

68 Denitrification in agricultural soils is a major source of N_2O, accounting for more than 60% of
69 the global anthropogenic emissions (20,21). A steady increase in atmospheric N_2O has been
70 recorded since the start of industrialization, largely driven by increasing and excessive use of
71 synthetic fertilizers (22,23) and these emissions are predicted to continue to increase unless
72 novel mitigation options are developed (24,25).

73 Although the addition of reactive nitrogen compounds via synthetic fertilizers accounts for
74 the main part of the N_2O emissions from agricultural soil, the N_2O emitted from legume
75 cropped fields is far from negligible. A compilation of data from ca 70 legume cropped fields
76 estimated ca 1.29 kg N_2O-N ha^{-1} during one growing season, while the corresponding data for
77 N-fertilized crops and pastures showed emissions of 3.22 kg N_2O-N ha^{-1} (26). Legumes do not
78 have to rely on uptake of reactive N such as NH_4^+ or NO_3^- but can acquire N through their
79 symbiotic relationship with some groups of bacteria, collectively called rhizobia, that elicit the
80 production of root nodules on the plant in which they fix atmospheric N_2. In this process, the
81 rhizobia reduce N_2 to NH_3 and the plant cells reduce the NH_3 further to glutamine which they
82 use to produce amino acids and eventually proteins (27). When this N-rich plant material is
83 degraded, organic N is released and mineralized to NH_3/NH_4^+ which will be oxidized to NO_3^- by
84 nitrifying organisms. The O_2 consumption by the nitrifiers, together with the production of NO_3^-
85 and the availability of organic compounds from the degraded plants, creates conditions that are
86 conducive to denitrification. A novel approach to minimize N_2O emissions from agricultural soil
87 is to enhance the populations of N_2O reducing bacteria (25). In the case of legume crops, which
88 are often inoculated with rhizobia to optimize the N_2-fixation, there are a few promising studies

89 reporting decreased N_2O emissions from soybean fields inoculated with rhizobia with the dual
90 capability of efficient N_2 fixation and N_2O reduction (28,29).

91 Based on this, selection of rhizobial strains for development of commercial inoculants
92 should, ideally, take both these aspects into account. One problem is, however, that far from all
93 rhizobia carry the *nosZ* gene that encodes Nos. There are relatively few surveys of
94 denitrification genes in different groups of rhizobia. Complete denitrification, which includes all
95 four reduction steps of NO_3^- to N_2, has so far mainly been reported for the genus
96 *Bradyrhizobium*, which is the microsymbiont of a range of economically important legume
97 crops such as soybean, cow pea and peanut (30,31). A full set of denitrification reductases in
98 bradyrhizobia include, with few exceptions, the periplasmic NO_3^- reductase Nap; the Cu-
99 containing NO_2^- reductase NirK, the *bc*-type NO reductase cNor and a NosZ belonging to clade I
100 (19,32). We recently investigated the denitrification capacity of bradyrhizobia from two strain
101 collections, one obtained from nodules of legume trees and herbs growing in Ethiopia, the
102 other mainly consisting of strains isolated from nodules of peanut growing in China (18,19). In
103 these collections, 50 and 37% of the isolates, respectively, were complete denitrifiers, while the
104 others generally lacked NosZ and thus were potential N_2O sources. Common to all strains with
105 complete denitrification was a strong preference for N_2O- over NO_3^- reduction. Transcription
106 analysis and proteomics showed comparable expression levels of Nap and Nos, suggesting a
107 control mechanism at the metabolic level where the electron pathway to Nos, which receives
108 electrons from cytochrome *c* via the *bc1* complex, competes very efficiently with the electron
109 pathway to Nap which goes via the membrane bond NapC.

110 The results presented in (18,19) were based on experiments with organisms provided with
111 ample amounts of C substrate (electron donor), which is likely to reflect the situation in legume
112 nodules where the microsymbiont receives C from the plant. It can, however, be expected that
113 rhizobia, which may survive for many years in soil (33), spend a large part of their life cycle as
114 free-living organisms in soil where they will experience lack of available C substrate most of the
115 time (2). Rhizobial inoculants that carry NosZ are thus potentially important sinks for N_2O
116 produced both by themselves and by other soil microbes. It is, however, not known if the
117 competition for electrons favoring N_2O reduction in well-fed cultures is retained during
118 substrate limitation ("starvation"). Here we exposed cultures of *Bradyrhizobium* strain HAMBI
119 2125, also studied in (19), to shorter and extended periods of starvation and analyzed the
120 denitrification kinetics, including the electron flow rates to the individual denitrification
121 reductases. We also quantified the cellular abundancies of Nap, Nir and Nos. The results have
122 practical implications, supporting that these organisms can act as sinks for N_2O under natural
123 conditions. Moreover, the results are ecologically interesting since they show that cultures
124 exposed to extended starvation divided into two opposite denitrification phenotypes, one with
125 very slow metabolism, the other with retained metabolism, possibly reflecting a strategy to
126 increase the chances for survival during periods of starvation.

127

128 **Results**

129 **Denitrification kinetics in cultures prepared following Bioassay 1.** Two bioassays were
130 developed for starvation experiments, Bioassay 1 and 2 (Figs. 1A and B). In a first experiment,
131 the denitrification gas kinetics, concentrations of NO_3^- and NO_2^- and electron flow rates to the

132 different reductases were compared for well-fed *vs* starved cultures (Figs. 2A-D). For this, the
133 starved cultures were prepared following Bioassay 1 (Fig. 1A), in which the cultures were
134 allowed to synthesize the denitrification reductases in the presence of ample amounts of
135 substrate. Cultures were raised under fully oxic conditions in YMB medium, after which the
136 headspace was made hypoxic to allow transition to anaerobic respiration in response to a
137 gradual depletion of oxygen. After centrifugation/washing, pellets were pooled and inoculated
138 into flasks containing YMB (9.9E+08 cells flask^{-1}) or buffer (5.0E+09 cells flask^{-1}), supplemented
139 with 1 mM KNO_3 and 0.25 mM KNO_2, and with He plus 1 ml N_2O (around 80 µmol N) in
140 headspace.

141 The initial O_2 concentration, which was 0.5 µM in cultures with YMB and 0.2 µM in cultures
142 with buffer, was depleted within the first 5 h in both treatments (insets in Figs. 2A and B). The
143 provided NO_2^- and N_2O were reduced simultaneously from the beginning of the incubation in
144 both treatments. The NO_3^- was left untouched in the well-fed cultures until the exogenous N_2O
145 was reduced (Fig. 2A), also seen from lack of electron flow to Nap except for a small peak in
146 electron flow early in the anoxic incubation (Fig. 2C). No NO_3^- reduction took place in the
147 starved cultures throughout the entire incubation period, as seen from the lack of electron flow
148 to Nap (Fig. 2D). The negative V_{eNap} estimated for the starved cultures (inset in Fig. 2D) and the
149 initial phase of the well-fed cultures are probably due to minor errors in calibration of N-gas
150 measurements as well as in parameters used to calculate rates of N-transformation (sampling
151 loss and N_2-leakage, see Molstad et al. (34)), which amounts to substantial errors in the
152 estimates of NO_3^-reduction rates because they are based on N-mass balance (explained in detail
153 by Lim et al. (35)). This implies a relatively high detection limit for NO_3^- reduction, and the

154 negative values cannot be taken as evidence for the complete absence of any electron flow to
155 NO_3^-. However, the measured NO concentrations lend some support to the claim that V_{eNap} was
156 ~0 until depletion of the externally provided N_2O. In the well-fed culture, the concentration of
157 NO declined to zero in response to depletion of NO_2^-, and increased soon after, as V_{eNap}
158 increased (Figs. 2A and C). Likewise, the NO concentration declined to very low values in
159 response to depletion of NO_2^- in the starved culture (Fig. 2B).

160 Fig. 2C and D show the calculated electron flow rates per cell to the individual reductases,
161 and their sum, illustrating their competition for electrons. This shows that the well-fed cells
162 (Fig. 2C) sustained a nearly constant total electron flow rate around 9 fmol e^- $cell^{-1}$ h^{-1}
163 throughout, but allocated to different reductases depending on the availability of electron
164 acceptors: As long as NO_2^- and N_2O were both present, Nos captured around 50% of the
165 electrons ($V_{eNos} \sim V_{eNir} + V_{eNor}$), increasing to 100% when NO_2^- was depleted after 6-7 hours,
166 while the electron flow rate to Nap remained insignificant until the externally provided N_2O
167 became depleted. The starving cells (Fig. 2D) had an order of magnitude lower total electron
168 flow rate per cell, declining gradually throughout the incubation, and here Nos captured >> 50%
169 of the electrons during the first 10 h ($V_{eNos} >> V_{eNir} + V_{eNor}$), but declined to ~50% towards the
170 end.

171 Bioassay 1 was also used in a second experiment, but in this case the cultures were
172 incubated anoxically ([O_2] <0.21 ±0.04 µM) in buffer containing only one of the N-oxides (NO_3^-,
173 NO_2^- or N_2O) as initial electron acceptor (Figs. 3A-C). This experiment established that starved
174 cultures readily reduced NO_3^- from the start when no other N-oxide was provided (Fig. 3A). It
175 also demonstrated that the cell specific electron flow to N-oxides was practically unaffected by

176 the type of electron acceptor provided, except for the slightly lower rates initially for flasks with
177 NO_2^-. For all treatments, the cell specific electron flow rate decreased gradually throughout,
178 and the levels are very similar to those observed in the first experiment (Fig. 3D).
179
180 **Cell size and PHA accumulation of starved vs well-fed cultures.** The morphologies of single
181 bacterial cells from different treatments (starved/well-fed and anoxic/oxic) were analyzed by
182 phase contrast microscopy (Fig. S1A). By quantifying cell dimensions, we found marginal but
183 statistically significant effects (Mann-Whitney test, $p < 0.01$) of starvation: while there was no
184 significant difference in cell area of individual cells (Fig. S1B), starved cells were on average
185 ~12% longer and ~5% thinner than well-fed cells (Fig. S1B). By further calculating cell volumes, a
186 slight reduction in average cell volume was observed upon starvation of aerobic cells ($p=0.057$),
187 but not for cells grown under anoxic conditions (Fig. S1C). Furthermore, a qualitative analysis of
188 the presence of PHA granules was done by staining the cells with Nile Red, a lipophilic dye with
189 high affinity for PHA (36). Large foci corresponding to PHA granules were seen in all conditions.
190 It should be noted that, as a lipophilic dye, Nile Red will also bind non-specifically to lipids and
191 membrane, and based on the imaging performed here, it could not be concluded whether there
192 were any significant differences in PHA content between the conditions.
193
194 **Denitrification kinetics after providing starving cultures with an artificial electron donor.**
195 An experiment was then performed in which TMPD plus ascorbate was added to starved
196 cultures (Bioassay 1), to provide cytochrome *c* with an excess of electrons (37,38). Since
197 cultures treated according to Bioassay 1 were able to provide electrons for denitrification (10-

198 18% of the electron flow in well-fed cells during the first 5 h, then decreasing to ca 4%; Fig. 2D),
199 we expected that the TMPD treatment would reduce or eliminate the oxidation of quinol by the
200 *bc1* complex and that this would allow electrons to flow to Nap via NapC, resulting in NO_3^-
201 reduction. We also expected that loading cytochrome *c* with electrons would relieve or weaken
202 the competition for electrons between Nir, Nor and NosZ. The results (Fig. 4) lend little support
203 to the former since the electron flow to Nap remained insignificant until N_2O had been
204 depleted. But the results confirm an effect of TMPD on the competition between Nos and Nir:
205 V_{eNir}, V_{eNor} and V_{eNos} were similar and high (4-5 fmol e^- $cell^{-1}$ h^{-1}) until NO_2^- was depleted. Thus,
206 Nir and Nos competed equally well when the cytochrome *c* pool was fully reduced by TMPD.
207 After depletion of NO_2^-, V_{eNos} leaped to its maximum level, 13-14 fmol N $cell^{-1}$ h^{-1}, and kept this
208 rate until all the exogenous N_2O was depleted.
209
210 **Denitrification kinetics and reductase abundancies of cultures exposed to extended**
211 **starvation following Bioassay 2.** While Bioassay 1 successfully induced starvation in terms of a
212 downshift in respiration, the rates did not reach a stable level during the assay but declined
213 gradually throughout, apparently approaching more stable low levels after 20 h. On this
214 background, we introduced a more severe starvation assay (Bioassay 2, Fig. 1B) by including a
215 20 h aerobic incubation in buffer prior to the starvation-denitrification assay, in order to reach a
216 lower and more stable rate of respiration than in the first experiment. In addition, Bioassay 2
217 was designed to force the cells to synthesize the denitrification proteome while starving. In
218 several preliminary experiments with Bioassay 2 (results not shown), we found a conspicuous
219 variability between flasks regarding the cell specific respiration rate where one or two out of

220 three replicate flasks had four to six times higher cell respiration rates than the other(s). At first,
221 we suspected that it could be due to impurities of flasks or magnets, but meticulous acid
222 washing failed to remove the stochastic variation. Being convinced that the stochasticity
223 reflects a real regulatory switch of the cultures, we performed a final experiment in which 15
224 replicate flasks were monitored for denitrification kinetics (Fig. 5).

225 The cultures received initially 1 mM NO_3^- in the buffer (but no NO_2^-), and He plus 1 ml N_2O
226 (80 µmol N) in headspace. The O_2 concentration at the time of inoculation was <0.5 µM in the
227 liquid. The flasks separated into two distinct denitrification phenotypes (Figs. 5A and B). Nine
228 flasks showed "low" cell specific respiration rates (total electron flow maximum 0.27 fmol e^-
229 $cell^{-1}$ h^{-1}), corresponding to approximately 2.7% compared to well-fed cultures (Fig. 5A), while
230 the other six showed a "fast" respiration rate (total electron flow 1.0-1.8 fmol e^- $cell^{-1}$ h^{-1}). Both
231 phenotypes reduced N_2O from the beginning of the incubation, showing a strong preference for
232 N_2O over NO_3^-. In the flasks with fast respiration, the cells started to reduce NO_3^- in response to
233 depletion of the externally provided N_2O. In the flasks with slow respiration, N_2O was not
234 depleted within the time frame of the experiment, and NO_3^- reduction remained negligible.

235 To investigate if cell lysis, and thus release of available C, could explain why some cultures
236 showed the "fast" growth phenotype, we compared the OD_{600} and the number of viable cells in
237 "slow" *vs* "fast" cultures. The samples were taken after incubation for 3.1 h in anoxic buffer,
238 when the two phenotypes were clearly distinct but when some possible growth of cells in the
239 "fast" cultures would not yet hide if lysis had occurred. The OD_{600} spanned from 0.12-0.13 with
240 no statistical difference ($p>0.3$) between cultures with "fast" and "slow" respiration. Similarly,
241 no difference ($p=0.4$) was found for the viable counts which showed 1.21E+10 to 1.33E+10 CFU

242 flask^{-1} for the “fast” cultures and 1.23E+10 to 1.34E+10 CFU flask^{-1} for the “slow” cultures (Fig.
243 S2).

244 We also tested the metabolic integrity of the cells in the flasks with slow respiration by
245 injecting C-substrates (YMB) to the flasks after 24.8 hours, which proved their capacity to
246 quickly regain activity approaching that of well-fed cells (Fig. 5A). To investigate if the observed
247 divergencies in phenotypes were due to differences in denitrification reductase abundancies,
248 we quantified the relative abundances of Nap, NirK and NosZ in samples taken at different time
249 points throughout the incubations (Figs. 5E and F), together with the corresponding
250 denitrification kinetics (Figs. 5A and B) and cell specific electron flow to reductases (Figs. 5C and
251 D). The membrane-bound NO reductase (cNor) could not be extracted quantitatively (the
252 results showed 1000 times lower abundancies than for the other denitrification reductases) and
253 is therefore not shown. The inoculum had been cultured aerobically for 3-4 generations, never
254 permitting the OD_{600} to exceed 0.1, to secure that any denitrification enzymes would be diluted
255 to extinction by aerobic growth, assuming that the transcription of all genes is effectively
256 repressed by oxygen. This strategy was apparently successful since Nap and Nir were
257 undetectable at the start of the anoxic incubation. NosZ, on the other hand, was detected also
258 in the aerobic cultures, suggesting that the *nosZ* gene is constitutively transcribed at low levels
259 in these organisms.

260 After transferring the cells to anoxic buffer, the abundance of all three reductases increased
261 both in cultures with “slow” and “fast” respiration. Cultures with “slow” respiration rate
262 synthesized less denitrification reductases than those with “fast” respiration rate during the
263 first 20 h. The relative abundances of the different reductases also differed between the two

264 phenotypes. In cultures with “slow” respiration, NosZ was significantly more abundant than
265 Nap and Nir ($p<0.01$), which were comparable (Fig. 5E). Cultures with “fast” respiration instead
266 contained higher abundancies of NosZ and Nir compared to Nap at 5 h. After this, the
267 abundance of Nir increased more than that of the others and at 20 h the LFQ of Nir was 0.20 ±
268 0.07, while the abundancies of NosZ and Nap were approximately half of that (Fig. 5F). After
269 addition of carbon substrate to the cultures with “slow” respiration, a rapid synthesis of all
270 three reductases took place. This synthesis was most prominent for Nir which, after a couple of
271 hours, had increased three-fold, reaching a relative abundance that was twice as high as Nap
272 and NosZ (Fig. 5E), resembling the abundance profile of the cultures with “fast” respiration (Fig.
273 5F).
274
275 **Discussion**
276 Detailed eco-physiological studies during the past decades have revealed several aspects of
277 how the denitrification process is regulated in different organisms (6,13,39). Most of this
278 knowledge is, however, based on laboratory studies where cultures have been grown under
279 optimal conditions, while less attention has been paid to understanding how denitrification,
280 and particularly the release of N_2O, is affected if cells are starved, which is the normal state of
281 cells in most natural environments. We focused on how starvation, i. e. lack of carbon substrate,
282 affects denitrification and N_2O release. The general notion has been that N_2O reductase is less
283 competitive for electrons than the other denitrification reductases, leading to emissions of N_2O
284 when the availability of electron donors is low. This is largely based on a single study of
285 *Alcaligenes faecalis* (40) and has been supported by some studies of complex communities but

286 contested by others (41-43). *A. faecalis* can perform partial denitrification reducing NO_2^- to N_2
287 using NirK, cNor and NosZ clade I, but this organism lacks dissimilatory NO_3^- reductases (Nar or
288 Nap). The study by Schalk-Otto (40), performed in continuous cultures, showed increased N_2O
289 release under low substrate concentrations, and it was suggested that N_2O reductase did not
290 compete successfully with the other reductases for electrons from cytochrome *c*, possibly due
291 to lower affinity for the electron donor. This conclusion needs, however, further verification by
292 more detailed studies of the mechanism involved. Moreover, such studies need to be extended
293 to other groups of denitrifying microorganisms and should include organisms carrying a
294 complete denitrification pathway (thus with Nar and/or Nap). Research over the past decades
295 has revealed diverse denitrification phenotypes among even closely related bacteria, with
296 implications for their accumulation of denitrification intermediate products (15,44).

297 The phenotype described for a range of taxonomically diverse *Bradyrhizobium* strains with a
298 complete denitrification pathway is characterized by a strong preference for N_2O over NO_3^-
299 when grown in full-strength YMB medium under denitrifying conditions (18,19). The present
300 study provides compelling evidence that this preference is retained when the organisms are
301 starved for carbon and energy, with practically no electron flow to Nap when N_2O was present
302 (Figs. 2A-D). This was not due to too low levels of Nap since the cultures showed well-
303 functioning Nap activity if NO_3^- was provided as the only initial electron acceptor (Fig. 3A).
304 Further evidence for this was obtained from the proteomics results, which showed that the
305 cultures, even when grown under more severe starvation conditions using Bioassay 2, were
306 able to produce comparable amounts of Nap, Nir and Nos (Figs. 5E and F). Therefore, the lack of
307 NO_3^- reduction during the period when there was N_2O in the system could not be explained by a

308 lack of Nap molecules. Instead, the results suggest the same metabolic-level phenomenon as
309 found for well-fed cultures in this study (Fig. 2A) and earlier (18,19), where NosZ outcompetes
310 Nap for electrons, leaving Nap virtually without electrons so long as exogenous N_2O is available.

311 The attempt to tweak the electron flow toward Nap by the addition of TMPD and ascorbate
312 did not result in measurable NO_3^- reduction in the starved cultures (Fig. 4A). A recent study by
313 Mania et al. (18) demonstrated that well-fed *Bradyrhizobium* cells did reduce some NO_3^- in the
314 presence of N_2O, if provided with TMPD and ascorbate. This suggested that NosZ (as well as Nir
315 and Nor) received electrons from strongly reduced cytochrome *c*, thus bypassing the electron
316 flow via the *bc1* complex, which allowed Nap to receive electrons from quinol, delivered from
317 the TCA cycle. The specificity of the electron delivery from TMPD to cytochrome *c* cannot be
318 taken for granted, however, and the result by Mania et al. (18) could instead reflect a minimum
319 of electron flow from TPMD to quinon or to NapC, directly, or indirectly. In the present
320 experiment with starved cells, TMPD + ascorbate failed to induce measurable electron flow to
321 Nap in the presence of N_2O (Fig. 4B). This probably reflects the marginal electron flow from the
322 TCA cycle to the quinon/quinol pool due to starvation. A separate experiment supported this,
323 showing that when carbon substrate (YMB) was added to starved cultures, this provided
324 enough electrons to support some Nap activity, although NosZ activity still dominated (Fig. S3).

325 At the same time, the result refutes the concerns regarding unspecific electron delivery of
326 electrons from TMPD to quinon. Functional Nap was apparently present, and NO_3^- reduction
327 started when N_2O was almost depleted, with V_{eNap} being 2 fmol e^- $cell^{-1}$ h^{-1} which was twice as
328 high as $V_{eNir/Nor}$ (Fig. 4B). The latter is as expected, since the reduction of 1 mole of NO_3^- to NO_2^-
329 requires 2 mole electrons, while reduction of NO_2^- and NO requires 1 mole electrons.

330 Furthermore, the electron flow to NosZ was the same as to Nir and Nor, suggesting that Nir and
331 NosZ competed equally well for electrons from cytochrome *c*. The maximum total electron flow
332 of 13-14 fmol e^- $cell^{-1}$ h^{-1} when the cytochrome *c* pool was saturated with electrons from TMPD
333 is likely to be close to the maximum capacity of the denitrification pathway. This electron flow
334 rate is higher than the total electron flow rate in the well-fed cells, which was 8-10 fmol e^- $cell^{-1}$
335 h^{-1} (Fig. 2C). The factor limiting V_{eNos} to 13-14 fmol $cell^{-1}$ h^{-1} is plausibly the rate of electron
336 delivery from cytochrome *c* and/or k_{cat} for Nos.

337 In another experiment we added YMB medium to "slow respiration" phenotypes of the
338 cultures that had been exposed to extended starvation (Figs. 5A, C and E). These cultures had
339 some NosZ activity (V_{eNos} 0.1-0.3 fmol e^- $cell^{-1}$ h^{-1}), while Nap and Nir activities could not be
340 detected. Addition of the electron donor (YMB) led to an immediate upshoot in the activities of
341 all reductases. This could not have been the case if the reductases were not present already,
342 which was proven by the proteomics results. Taken together, the results support that the
343 absolute preference for N_2O over NO_3^- was due to competition for electrons, also under severe
344 starvation conditions.

345 It is well known that bacteria have developed a range of physiological responses to tackle
346 starvation. Some survive by forming spores, but most bacteria survive by strongly reduced
347 metabolic rates and minimizing the synthesis of some proteins while upregulating others such
348 as genes for high-affinity transporters, essential repair mechanisms and alternative energy
349 sources (3,45,46). Some such changes have been observed in rhizobia belonging to *Rhizobium*
350 *leguminosarum*, which stayed viable for long periods (55 days) of C starvation (47). Changes in
351 cell size are common during long-term starvation, sometimes leading to the formation of small

352 or even ultra-microcells which may have increased tolerance to antibiotics and other stresses
353 (2,46). Another way for many bacteria, including rhizobia, to survive is to use carbon stored as
354 polyhydroxyalkanoates (PHA) or glycogen, formed during periods of ample nutrient abundance
355 (48). In the present study, the metabolic activity, measured as anaerobic respiration rate,
356 decreased to between 1 and 18% that of well-fed cultures, depending on which starvation
357 bioassay was used. We did not, however, detect any obvious decrease in cell size when
358 comparing cells starved for 24 h, although cell morphologies were slightly altered (Figs. S1A and
359 B). PHA was observed in the starved cells as well as well-fed ones, as shown with Nile red
360 staining (Fig. S1A) and no obvious reduction in PHA could be observed during starvation from
361 our assays. Since this was a comparably short period of starvation, it is conceivable that the
362 cells would make use of the stored carbon if the starvation was prolonged. It could be
363 speculated that one reason for not using the PHA reserves (and glycogen) immediately, is that
364 these are saved to be used during bacteroid formation (48). To clarify these issues, more
365 detailed studies are however needed.

366 A striking separation into two phenotypes during starvation, as shown in Fig. 5, was
367 observed in repeated experiments (Bioassay 2), each time with about two thirds of the flasks
368 showing a "fast" and the others "slow" respiration: 1.0-1.8 fmol e^- $cell^{-1}$ h^{-1} vs 0.1-0.3 fmol e^-
369 $cell^{-1}$ h^{-1}, respectively. Phenotypic heterogeneity has been observed in single-strain cultures of
370 various bacteria when exposed to carbon substrate deficiency and may, or may not, be due to
371 mutations during starvation for one week or more (3,49). Mutations in the entire population in
372 several replicate flasks are unlikely and cannot, however, have caused the rapid diversification
373 into "slow"- or "fast" respiration in the present study. It may instead reflect a stochastic

374 phenomenon, or that the culture contained different subpopulations. We speculated that the
375 "fast respiration" phenotype may be due to a fraction of the cells dying, allowing the other cells
376 to survive on nutrients released from lysed cells, as seen for other bacteria (3). However, this
377 would require lysis of a substantial fraction of the cells, which is refuted by the observation that
378 the flasks with "slow" and "fast" phenotypes had practically identical numbers of viable cells
379 (Fig. S2). Thus, further studies are needed to understand this phenomenon of different
380 respiration rates.

381 Although the starvation bioassays developed for this study cannot be regarded as a close
382 mimicking of the conditions in natural environments, it is conceivable from the experiments
383 that these organisms are potentially strong sinks for N_2O when living in soil under fluctuating
384 availability of carbon substrate. Bioassay 1 is probably closer to a "real-world" situation than
385 Bioassay 2, since it is likely that denitrifying bacteria experience regular fluctuations in oxygen
386 and thus are not devoid of denitrification reductases if they enter starvation. On the other hand,
387 Bioassay 2, where the cells had to produce the denitrification proteome in the absence of
388 external electron donors (C-substrate), showed that even under these conditions N_2O reduction
389 strongly dominated over NO_3^- reduction.

390

391 **Materials and methods**

392 **Bacterial strain and culture preparations.** *Bradyrhizobium* strain HAMBI 2125, originally
393 isolated from nodules of *Arachis hypogaea* growing in Sichuan, China (50), was used in all
394 experiments. This strain, which is closely related to *Bradyrhizobium ottawaense*, contains the
395 genetic set-up for complete denitrification (19). A culture was raised from one single colony

396 after streaking on agar plates. After checking the purity by sequencing the 16S rRNA gene (19),
397 portions were preserved in 15% glycerol at -80 °C. Cultures for all the experiments were started
398 from the -80 °C stocks and raised under fully oxic conditions in 120 ml serum flasks containing
399 50 ml Yeast Mannitol Broth (YMB): 10 g l^{-1} D-Mannitol, 0.5 g l^{-1} K_2HPO_4, 0.2 g l^{-1} $MgSO_4 \cdot 7H_2O$,
400 0.1 g l^{-1} NaCl and 0.5 g l^{-1} yeast extract (51). All incubations were done at 28 °C. Medical flasks
401 (120 ml) were used in all experiments. A magnet in each flask secured vigorous stirring (600-
402 700 rpm) to avoid cell aggregation and to optimize the gas exchange between liquid and gas
403 phases (18). To prevent that the cells experienced anoxia during this oxic incubation, and thus
404 to avoid de novo synthesis of denitrification reductases, portions were regularly transferred to
405 new flasks containing fresh medium, so that the OD_{600} was never allowed to exceed 0.1 (19).
406 These aerobically grown cultures were used as inoculants in the "starvation bioassays"
407 described below.

408 Flasks for cultures incubated under hypoxic conditions were prepared as described in (18).
409 Briefly, flasks (120 ml) containing 50 ml buffer (or medium) were capped with sterilized, gas
410 tight butyl rubber septa (Matrix AS, Norway). The air was removed by applying vacuum
411 repeatedly (6 x 360 s) and He was then filled for 30 s, after which the overpressure was
412 released. The flasks were left for two days to equilibrate the gases between the headspace and
413 liquid (52). Then, 0.7 ml or 1 ml O_2 (equal to 1 or 1.5 vol %) and 1 ml N_2O (70 to ~80 µmol N
414 $flask^{-1}$) was injected into the headspace and sterile filtered solutions of KNO_3 (and sometimes
415 KNO_2) were added to the liquid reaching initial, desired concentrations (0.25 -1 mM).
416

417 **Starvation bioassays.** Starvation bioassays were established, which followed one of the
418 procedures described in Fig. 1. In Bioassay 1 "Mild starvation", cultures were allowed to make
419 the transition to denitrification in full-strength YMB before being exposed to starvation. Oxically
420 grown, well-fed cultures were incubated for 48 h after which the headspace was replaced by He
421 and 1% O_2, and 1 mM KNO_3 was added to the medium. When O_2 was depleted, the cultures
422 were centrifuged (10 000 × g at 4 °C for 10 min) and washed twice in sterile ddH_2O. The pellets
423 (triplicates) were pooled to reduce bias in the form of variations due to the
424 centrifugation/washing. Each pellet was divided into three and used to inoculate anoxic flasks
425 containing 50 ml C-free buffer supplemented with 1 mM KNO_3 and 0.25 or 0.5 mM KNO_2 and
426 with He and/or 1 ml N_2O (around 80 µmol N $flask^{-1}$) in the headspace. When incubated in the
427 buffer, the respiration rate of the cultures was 10-18% that of well-fed cultures during the first
428 15 h, then it decreased to about 4%.

429 In Bioassay 2 ("extended starvation"), denitrification was instead induced after having
430 exposed the cells to starvation for 20 h. The cultures were raised in fully oxic flasks containing
431 YMB medium. When OD_{600} reached ~0.1, the cultures were centrifuged (10 000 × g at 4 °C for
432 10 mins) and washed twice in sterile ddH_2O. The pellets (triplicates) were pooled after which
433 they were evenly divided and used to inoculate fully oxic flask containing C-free "starvation
434 buffer". These cultures were incubated for 20 h, then centrifuged after which the pellets were
435 pooled and divided evenly before being inoculated into flasks containing C-free "starvation
436 buffer" with 1 mM KNO_3, and with He and 1 ml N_2O (around 80 µmol N $flask^{-1}$) in headspace.
437 The respiration rate of cultures exposed to "extended starvation" was ca 1-4% compared to
438 that of well-fed cultures. Results from the different starvation bioassays were compared to

439 those from well-fed cultures. To avoid biases, the treatments, which were in all cases set up at
440 least in triplicates (n ≥ 3), were the same regarding centrifugations and washings until the last
441 step when pooled cells were inoculated to anoxic flasks containing either YMB or buffer. The
442 carbon source in the YMB medium comprised >200 times surplus of electron donor compared
443 to electron acceptors throughout all incubations, thus ensuring that the electron donor was not
444 depleted. All cultures were incubated at 28°C, and with vigorous stirring (600-700 rpm).
445
446 **Addition of YMB medium or TMPD as electron donors to starved cultures.** Experiments
447 were performed to investigate how starved cultures of *Bradyrhizobium* strain HAMBI 2125
448 responded to the addition of an electron donor, either provided as an artificial electron donor
449 (Fig. 4) or as YMB medium (2 ml mannitol /yeast solution providing them with a substrate
450 concentration corresponding to half-strength YMB, thus 5 g mannitol and 0.25 g yeast l^{-1}, Fig. 5).
451 As artificial electron donor we used sodium TMPD (N, N, N´, N´-tetramethyl-p-
452 phenylenediamine) which, in the presence of ascorbate, donates electrons to cytochrome c
453 thus providing electrons to Nir and NosZ (18,37). Ascorbate and TMPD (both from Sigma-
454 Aldrich®, Germany) were dissolved in ddH_2O or 96% ethanol, respectively, and filter sterilized.
455 The solutions were added to the incubation flasks 10-15 mins before gas sampling. The effect of
456 different concentrations of TMPD (100, 250, and 500 µM in the culture buffer) combined with
457 10 mM ascorbate on N_2O reduction was checked prior to the main experiments. This showed
458 that 500 µM TMPD had an obvious inhibition effect on N_2O reduction, while 100 µM and 250
459 µM showed no inhibitory effect (not shown). To minimize other, possible effects we used 100
460 µM TMPD for the experiments (as done in Mania et al. (18)). In another experiment, shown in

461 Fig. S3, 4 ml of a mannitol/yeast solution was added to flasks containing 50 ml starved cultures,
462 providing them with a substrate concentration corresponding to full strength YMB (10 g
463 mannitol and 0.5 g yeast l^{-1}).
464
465 **Monitoring of gas kinetics, NO_3^- and NO_2^- concentrations and electron flow rates.** The
466 culture flasks were placed in a robotized incubation system and the headspace gas was sampled
467 frequently for N_2, N_2O, NO and O_2 measurements (34). Gas losses caused by sampling were
468 taken into account when calculating the production and consumption of gases, as described by
469 Molstad et al. (34) and Mania et al. (18). The concentration of O_2 in the anoxic incubation flasks
470 was <0.6 µM at the start of the experiment, which was well below the level for initiating
471 denitrification (4.6 µM; (19)).
472 The NO_2^- concentrations were monitored as described in Mania et al. (18). Briefly, samples
473 (0.1- 0.5 ml) were taken every 1 or 2 hours (n=3) from the liquid phase through the septum of
474 the flasks using a sterile syringe. To avoid that the gas kinetics was affected by the sampling, a
475 set of flasks was dedicated to NO_2^- measurements and a parallel set was left untouched for gas
476 measurements. NO_2^- was determined using a chemoluminescence NOx analyzer (Sievers NOA™
477 280i, GE Analytical Instruments) after at first reducing the NO_2^- to NO by adding 10 µl liquid
478 sample into a purging device containing a reducing agent (50% acetic acid with 1% (w/v) NaI)
479 (53,54). The NO_2^- concentrations were determined against a standard curve (range 0-2 mM
480 NO_2^-; r^2= 0.999).
481 The cell specific electron flow rates (V_e, mol e^- $cell^{-1}$ h^{-1}) for each time increment between
482 two gas samplings were calculated as $V_{eflask}(t)/(N(0)+E_{cum}(t)*Y)$, where $V_{eflask}(t)$ is the electron

483 flow rate in the flask (mol e^- $flask^{-1}$ h^{-1}) calculated from measurements, *N(0)* is number of cells in
484 the flask at time=0, $E_{cum}(t)$ is the cumulated electron flow (mol e^- $flask^{-1}$) at time=t , and Y is the
485 yield per mol electron (cells mol^{-1} e^-) for HAMBI 2125 as measured previously (19). The
486 conversion factor 5.8E8 cells ml^{-1} *$OD_{600}{}^{-1}$ was used to convert OD_{600} to cell numbers (19).
487
488 **Proteomics**. The abundances of Nap, Nir and NosZ were quantified in starved cultures
489 treated as described for Bioassay 2 (extended starvation). Altogether eighteen flasks were
490 prepared according to Fig. 1B. After the 20 h aerobic incubation in C-free buffer, three flasks
491 were harvested for proteomics analysis and, following centrifugation/washing, the three cell
492 pellets from these flasks were frozen individually at -20 °C. The cultures in the other flasks were
493 pooled three by three and after centrifugation/washing, each cell pellet was divided in three
494 and used to inoculate new flasks containing C-free buffer with NO_3^- in the liquid and with He
495 and 1 ml N_2O in the headspace (Fig. 1B). These flasks (fifteen in total) were placed in the robotic
496 incubation system for monitoring of gas kinetics and NO_2^- concentrations as described above.
497 The entire culture volume (50 ml) was harvested from each of triplicate flasks at different time
498 points during the anoxic incubation. The cultures in six of the flasks showed a "fast" respiration
499 rate (total electron flow 1.0-1.8 e^- $cell^{-1}$ h^{-1}) and were harvested at 5 and 20 h of incubation in
500 anoxic buffer (triplicates at each sampling point). The cultures in the other nine flasks showed a
501 "slow" respiration rate (maximum total electron flow rate was 0.27 fmol e^- $cell^{-1}$ h^{-1}). Six of
502 them were harvested in triplicates after 10 and 20 h in anoxic buffer. The remaining three flasks
503 from the cultures with "slow" respiration rate received a portion of YMB at 24.8 hand were
504 harvested at 27 h. Harvested cell cultures were centrifuged and stored as pellets at -20 °C. The

505 protein extraction was as described in Gao et al. (19). Briefly, the thawed cell pellets were
506 resuspended in lysis buffer (20 mM Tris–HCl pH 8, 0.1% v/v Triton X-100, 200 mM NaCl, 1 mM
507 DTT). They were then subjected to bead beating (3 × 45 s) with glass beads (particle size ≤ 106
508 µm; Sigma) using a MP Biomedicals™ FastPrep-24™ (Thermo Fischer Scientific) at maximum
509 power and with cooling on ice between the cycles. After centrifugation to remove cell debris
510 (10 000 × g; 5 min), the supernatant, containing water soluble proteins, was used for proteomic
511 analysis using an Orbitrap mass spectrometer (described in (19,55)). Quantification was based
512 on LFQ (label-free quantification) in MaxQuant (56), and the relative abundance of the
513 individual reductases was calculated as percentages of the sum of all protein abundances for
514 each time point. The nitric oxide reductases NorB/C were not measured since only a small
515 fraction of these membrane-bound enzymes can be accurately obtained with this extraction
516 protocol (approximately 1/1000th the quantity of the other reductases).
517
518 **Viable counts and microscopy.** The number of viable cells in starved cultures showing slow
519 and fast respiration rates, observed in flasks prepared according to Bioassay 2, was determined
520 by plating dilutions of the cultures on yeast-mannitol agar (YMA). The morphology of cells from
521 well-fed cultures and starved cultures was compared using phase contrast microscopy and a
522 qualitative determination (presence/absence) of PHA was done by staining with Nile Red
523 (Sigma-Aldrich) followed by fluorescence microscopy. Microscopy was performed on a Zeiss
524 AxioObserver with an Orca-Flash4.0 CMOS camera (Hamamatsu Photonics) controlled by the
525 ZEN Blue software. Images were taken with a 100x phase contrast objective. A HPX-120

526 Illuminator was used as light source for fluorescence microscopy. Images were prepared using
527 ImageJ and analysis of cell sizes was done using the ImageJ-plugin MicrobeJ (57).
528

529 **Acknowledgment**

530 This project was supported by Kingenta Ecological Engineering Group Co., LTD and by the
531 project PASUSI financed by the EC Horizon2020 ERA-NET Cofund Programme, Grant agreement
532 No. 727715 and by the Research Council of Norway, projects No. 290488 and 325770. Yuan Gao
533 is grateful to the China Scholarship Council (CSC) for financial support. We thank Gro Stamsås
534 for help with microscopy.
535

536 **References**

537 1. Hobbie JE, Hobbie EA. 2013. Microbes in nature are limited by carbon and energy: The
538 starving-survival lifestyle in soil and consequences for estimating microbial rates. Front
539 Microbiol 4:324.
540 2. Morita RY. 1990. The starvation-survival state of microorganisms in nature and its
541 relationship to the bioavailable energy. Experientia 46:813–817.
542 3. Bergkessel M, Basta DW, Newman DK. 2016. The physiology of growth arrest: Uniting
543 molecular and environmental microbiology. Nat Rev Microbiol 14:549–562.
544 4. Ratcliff WC, Kadam SV, and Denison, R.F. 2008. Poly-3-hydroxybutyrate (PHB) supports
545 survival and reproduction in starving rhizobia. FEMS Microbiol Ecol 65:391–399.

546 5. Müller-Santos M, Koskimäki JJ, Alves LPS, de Souza EM, Jendrossek D, Pirttilä AM. 2021. The
547 protective role of PHB and its degradation products against stress situations in bacteria.
548 FEMS Microbiol Rev 45:fuaa058.
549 6. Zumft WG. 1997. Cell biology and molecular basis of denitrification. Microbiol Mol Biol Rev
550 61:533–616.
551 7. Duffner C, Kublik S, Fösel B, Frostegård Å, Schloter M, Bakken L, Schulz S. 2022. Genotypic
552 and phenotypic characterization of hydrogenotrophic denitrifiers. Environ Microbiol
553 24:1887-1901.
554 8. Schneider LK, Wüst A, Pomowski A, Zhang L, Einsle O. 2014. No laughing matter: The
555 unmaking of the greenhouse gas dinitrogen monoxide by nitrous oxide reductase. Met Ions
556 Life Sci 14:177–210.
557 9. Hein S, Simon J. 2019. Bacterial nitrous oxide respiration: electron transport chains and
558 copper transfer reactions. Adv Microb Physiol 75:137–175.
559 10. Shapleigh JP. 2013. Denitrifying prokaryotes: Prokaryotic Physiology and Biochemistry. In
560 Rosenberg E, DeLong EF, Lory S, Stackebrandt E, Thompson F. (eds), The prokaryotes, pp.
561 405-425. Berlin, Heidelberg: Springer.
562 11. Graf DRH, Jones CM, Hallin S. 2014. Intergenomic comparisons highlight modularity of the
563 denitrification pathway and underpin the importance of community structure for N_2O
564 emissions. PLoS ONE 9:e114118.
565 12. Richardson D, Felgate H, Watmough N, Thomson A, Baggs E. 2009. Mitigating release of the
566 potent greenhouse gas N_2O from the nitrogen cycle - could enzymic regulation hold the key?
567 Trends Biotechnol 27:388-97.

568 13. Spiro S. 2012. Nitrous oxide production and consumption: regulation of gene expression by
569 gas-sensitive transcription factors. Philos Trans R Soc Lond B Biol Sci 367:1213-25.
570 14. Liu B, Frostegård Å, Bakken LR. 2014. Impaired reduction of N_2O to N_2 in acid soils is due to
571 a posttranscriptional interference with the expression of *nosZ*. mBio 5:e01383-14.
572 15. Liu B, Mao Y, Bergaust L, Bakken LR, Frostegård A. 2013. Strains in the genus *Thauera*
573 exhibit remarkably different denitrification regulatory phenotypes. Environ Microbiol
574 15:2816-28.
575 16. Gaimster H, Alston M, Richardson DJ, Gates AJ, Rowley G. 2018. Transcriptional and
576 environmental control of bacterial denitrification and N_2O emissions. FEMS Microbiol Lett
577 365:fnx277.
578 17. Lycus P, Soriano-Laguna MJ, Kjos M, Richardson DJ, Gates AJ, Milligan DA, Frostegård Å,
579 Bergaust L, Bakken LR. 2018. A bet-hedging strategy for denitrifying bacteria curtails their
580 release of N_2O. Proc Natl Acad Sci 115:11820–11825.
581 18. Mania D, Woliy K, Degefu T, Frostegård Å. 2020. A common mechanism for efficient N_2O
582 reduction in diverse isolates of nodule-forming bradyrhizobia. Environ Microbiol 22:17–31.
583 19. Gao Y, Mania D, Mousavi SA, Lycus P, Arntzen M, Woliy K, Lindström K, Shapleigh JP, Bakken
584 LR, Frostegård Å. 2021. Competition for electrons favours N_2O reduction in denitrifying
585 *Bradyrhizobium* isolates. Environ Microbiol 23:2244–2259.
586 20. Butterbach-Bahl K, Baggs EM, Dannenmann M, Kiese R, Zechmeister-Boltenstern S. 2013.
587 Nitrous oxide emissions from soils: How well do we understand the processes and their
588 controls? Philos Trans R Soc Lond B Biol Sci 368:20130122.

21. Thompson RL, Lassaletta L, Patra PK, Wilson C, Wells KC, Gressent A, Koffi EN, Chipperfield M, Winiwarter W, Davidson EA, Tian H, Canadell JG. 2019. Acceleration of global N_2O emissions seen from two decades of atmospheric inversion. Nat Clim Change 9:993–998.

22. Tian H, Lu C, Ciais P, Michalak AM, Canadell JG, Saikawa E, Huntzinger DN, Gurney KR, Sitch S, Zhang B, Yang J, Bousquet P, Bruhwiler L, Chen G, Dlugokencky E, Friedlingstein P, Melillo J, Pan S, Poulter B, Prinn R, Saunois M, Schwalm CR, Wofsy SC. 2016. The terrestrial biosphere as a net source of greenhouse gases to the atmosphere. Nature 531:225–228.

23. Tian H, Xu R, Canadell JG, Thompson RL, Winiwarter W, Suntharalingam P, Davidson EA, Ciais P, Jackson RB, Janssens-Maenhout G, Prather MJ, Regnier P, Pan N, Pan S, Peters GP, Shi H, Tubiello FN, Zaehle S, Zhou F, Arneth A, Battaglia G, Berthet S, Bopp L, Bouwman AF, Buitenhuis ET, Chang J, Chipperfield MP, Dangal, SRS, Dlugokencky E, Elkins JW, Eyre BD, Fu B, Hall B, Ito A, Joos F, Krummel PB, Landolfi A, Laruelle GG, Lauerwald R, Li W, Lienert S, Maavara T, MacLeod M, Millet DB, Olin S, Patra PK, Prinn RG, Raymond PA, Ruiz DJ, van der Werf GR, Vuichard N, Wang J, Weiss RF, Wells KC, Wilson C, Yang J, Yao Y. 2020. A comprehensive quantification of global nitrous oxide sources and sinks. Nature 586: 248–256.

24. Davidson EA, Kanter D. 2014. Inventories and scenarios of nitrous oxide emissions. Environ Res Lett 9:105012.

25. Bakken LR, Frostegård Å. 2020. Emerging options for mitigating N_2O emissions from food production by manipulating the soil microbiota. Curr Opin Environ Sustain 47:89–94.

609 26. Jensen ES, Peoples MB, Boddey RM, Gresshoff PM, Henrik HN, Alves BJR, Morrison MJ. 2012.
610 Legumes for mitigation of climate change and the provision of feedstock for biofuels and
611 biorefineries. A review. Agron Sustain Dev 32:329-364.
612 27. Poole P, Ramachandran V, Terpolilli J. 2018. Rhizobia: From saprophytes to endosymbionts.
613 Nat Rev Microbiol 16:291–303.
614 28. Hénault C, Revellin C. 2011. Inoculants of leguminous crops for mitigating soil emissions of
615 the greenhouse gas nitrous oxide. Plant Soil 346:289–296.
616 29. Itakura M, Uchida Y, Akiyama H, Hoshino YT, Shimomura Y, Morimoto S, Tago K, Wang Y,
617 Hayakawa C, Uetake Y, Sánchez C, Eda S, Hayatsu M, Minamisawa K. 2013. Mitigation of
618 nitrous oxide emissions from soils by *Bradyrhizobium japonicum* inoculation. Nat Clim
619 Change 3:208–212.
620 30. Jaiswal SK, Dakora FD. 2019. Widespread distribution of highly adapted *Bradyrhizobium*
621 species nodulating diverse legumes in Africa. Front Microbiol 10:310.
622 31. Woliy K, Degefu T, Frostegård Å. 2019. Host Range and Symbiotic Effectiveness of N_2O
623 Reducing Bradyrhizobium Strains. Front Microbiol 10:2746.
624 32. Bedmar EJ, Robles EF, Delgado MJ. 2005. The complete denitrification pathway of the
625 symbiotic, nitrogen-fixing bacterium *Bradyrhizobium japonicum*. Biochem Soc Trans 33:141-
626 144.
627 33. Narozna D, Pudełko K, Króliczak J, Golińska B, Sugawara M, Mądrzak CJ, Sadowsky MJ. 2015.
628 Survival and competitiveness of *Bradyrhizobium japonicum* strains 20 years after
629 introduction into field locations in Poland. Appl Environ Microbiol 81:5552–5559.

630 34. Molstad L, Dörsch P, Bakken LR. 2007. Robotized incubation system for monitoring gases
631 (O_2, NO, N_2O, N_2) in denitrifying cultures. J Microbiol Methods 71:202–211.
632 35. Lim NYN, Frostegård Å, Bakken LR. 2018. Nitrite kinetics during anoxia: The role of abiotic
633 reactions versus microbial reduction. Soil Biol Biochem 119:203–209.
634 36. Spiekermann P, Rehm BH, Kalscheuer R, Baumeister D, Steinbüchel A. 1999. A sensitive,
635 viable-colony staining method using Nile red for direct screening of bacteria that
636 accumulate polyhydroxyalkanoic acids and other lipid storage compounds. Arch Microbiol
637 171:73-80.
638 37. Kimelberg HK, Nicholls P. 1969. Kinetic studies on the interaction of TMPD with cytochrome
639 *c* and cytochrome *c* oxidase. Arch Biochem Biophys 133:327–335.
640 38. Bueno E, Richardson DJ, Bedmar EJ, Delgado MJ. 2009. Expression of *Bradyrhizobium*
641 *japonicum* cbb3 terminal oxidase under denitrifying conditions is subjected to redox control.
642 FEMS Microbiol Lett 298:20–28.
643 39. Torres MJ, Simon J, Rowley G, Bedmar EJ, Richardson DJ, Gates AJ, Delgado MJ. 2016.
644 Nitrous Oxide Metabolism in Nitrate-Reducing Bacteria: Physiology and Regulatory
645 Mechanisms. Adv Microb Physiol 68:353-432.
646 40. Schalk-Otte S, Seviour R, Kuenen J, Jetten MSM. 2000. Nitrous oxide (N_2O) production by
647 *Alcaligenes faecalis* during feast and famine regimes. Water Res 34:2080-2088.
648 41. Itokawa H, Hanaki K, Matsuo T. 2001. Nitrous oxide production in high-loading biological
649 nitrogen removal process under low COD/N ratio condition. Water Res 35:657-664.

650 42. Lu H, Chandran K. 2010. Factors promoting emissions of nitrous oxide and nitric oxide from
651 denitrifying sequencing batch reactors operated with methanol and ethanol as electron
652 donors. Biotechnol Bioeng 106:390-8.
653 43. Pan Y, Ni BJ, Bond PL, Ye L, Yuan Z. 2013. Electron competition among nitrogen oxides
654 reduction during methanol-utilizing denitrification in wastewater treatment. Water Res
655 47:3273-81.
656 44. Lycus P, Bøthun KL, Bergaust L, Shapleigh JP, Bakken LR, Frostegård Å. 2017. Phenotypic and
657 genotypic richness of denitrifiers revealed by a novel isolation strategy. ISME J 11:2219–
658 2232.
659 45. Kjelleberg S, Albertson N, Flärdh K, Holmquist L, Jouper-Jaan A, Marouga R, Ostling J,
660 Svenblad B, Weichart D. 1993. How do non-differentiating bacteria adapt to starvation?
661 Antonie Van Leeuwenhoek 63:333-41.
662 46. Gray DA, Dugar G, Gamba P, Strahl H, Jonker MJ, Hamoen LW. 2019. Extreme slow growth
663 as alternative strategy to survive deep starvation in bacteria. Nat Commun 10:890.
664 47. Thorne SH, Williams HD. 1997. Adaptation to nutrient starvation in Rhizobium
665 leguminosarum bv. phaseoli: analysis of survival, stress resistance, and changes in
666 macromolecular synthesis during entry to and exit from stationary phase. J Bacteriol
667 179:6894-901.
668 48. Lodwig EM, Leonard M, Marroqui S, Wheeler TR, Findlay K, Downie JA, Poole PS. 2005. Role
669 of polyhydroxybutyrate and glycogen as carbon storage compounds in pea and bean
670 bacteroids. Mol Plant Microbe Interact 18:67-74.

671 49. Chen H, Chen CY. 2014. Starvation induces phenotypic diversification and convergent
672 evolution in *Vibrio vulnificus*. PLoS One 9:e88658.
673 50. Zhang X, Nicki G, Kaijalaineni S, Terefework Z, Paulin L, Tighe SW, Graham PH, Lindström K.
674 (1999) Phylogeny and Diversity of *Bradyrhizobium* Strains Isolated from the Root Nodules of
675 Peanut (Arachis hypogaea) in Sichuan, China. Syst Appl Microbiol 22:378-386.
676 51. Schwartz W. 1972. Vincent, J.M. A Manual for the Practical Study of the Root-Nodule
677 Bacteria (IBP Handbuch No. 15 des International Biology Program, London). XI u. 164 S., 10
678 Abb., 17 Tab., 7 Taf. Oxford-Edinburgh 1970: Blackwell Scientific Publ., 45 s. Z Allg Mikrobiol
679 12:1521-4028.
680 52. Mania D, Heylen K, van Spanning RJ, Frostegård Å. 2016. Regulation of nitrogen metabolism
681 in the nitrate-ammonifying soil bacterium *Bacillus vireti* and evidence for its ability to grow
682 using N_2O as electron acceptor. Environ Microbiol 18:2937-50.
683 53. Cox RD. 1980. Determination of nitrate and nitrite at the parts per billion level by
684 chemiluminescence. Anal Chem 52:332–335.
685 54. MacArthur PH, Shiva S, Gladwin MT. 2007. Measurement of circulating nitrite and S-
686 nitrosothiols by reductive chemiluminescence. J Chromatogr B Analyt Technol Biomed Life
687 Sci 851:93–105.
688 55. Conthe M, Lycus P, Arntzen MØ, Ramos da Silva A, Frostegård Å, Bakken LR, Kleerebezm R,
689 van Loosdrecht MCM. 2019. Denitrification as an N_2O sink. Water Res 151:381–387.
690 56. Cox J, Mann M. 2008. MaxQuant enables high peptide identification rates, individualized
691 p.p.b.-range mass accuracies and proteome-wide protein quantification. Nat Biotechnol
692 26:1367-72.

693 57. Ducret A, Quardokus EM, Brun YV. 2016. MicrobeJ, a tool for high throughput bacterial cell
694 detection and quantitative analysis. Nat Microbiol 20:16077.

695

696 **Figure legends**

697 **FIG 1** Bioassays for assessing the effect of starvation on electron flow to denitrification enzymes.
698 A: Bioassay 1: starvation of cells with a previously expressed denitrification proteome. Cells
699 were raised from stock cultures in fully oxic flasks containing YMB medium. When OD_{600}
700 reached ~0.1, the flasks were made anoxic by He-washing, then supplemented with 1% O_2 in
701 the headspace and 1 mM NO_3^- in the liquid. The cultures were allowed to deplete the O_2 and to
702 initiate denitrification when growing in YMB medium, after which they were centrifuged (10
703 000 × g at 4 °C for 10 mins) and washed twice in sterile ddH_2O. The pellets from triplicate flasks
704 were pooled and used to inoculate flasks containing either C-free buffer or YMB medium (well-
705 fed control), in both cases supplemented with 1 mM KNO_3 and 0.25 or 0.5 mM KNO_2, and with
706 He and 1 ml N_2O (around 80 µmol N $flask^{-1}$) in headspace. The starving cells, incubated in buffer,
707 had a low respiratory electron flow rate (mol electrons $cell^{-1}$ h^{-1}), initially being 10-18 % that of
708 the well-fed cultures, and then decreasing to reach around 4% after 20 h. Results from
709 experiments using Bioassay 1 are presented in Figs. 2, 3 and 4.
710 B: Bioassay 2: denitrification induced during starvation. Cells were raised from stock cultures in
711 fully oxic flasks containing YMB medium. When OD_{600} reached ~0.1, the cultures were
712 centrifuged (10 000 × g at 4 °C for 10 mins) and washed twice in sterile ddH_2O. The pellets from
713 triplicate flasks were pooled, after which they were evenly divided and used to inoculate fully
714 oxic flasks containing C-free buffer. These cultures were incubated for 20 h, then centrifuged

715 after which the pellets were pooled and divided evenly before being inoculated into flasks
716 containing C-free buffer-provided with 1 mM KNO_3, and with He and 1 ml N_2O (around 80 µmol
717 N flask^{-1}) in headspace. The respiration rate (mol electrons cell^{-1} h^{-1}) of the starving cultures was
718 1-4% compared to that of well-fed cultures. All cultures in Bioassays 1 and 2 were incubated at
719 28°C, and with vigorous stirring (650 rpm). Results from experiments using Bioassay 1 are
720 presented in Figs. 5 and S2.

721

722 **FIG 2** Denitrification kinetics as affected by starvation in cultures with a complete denitrification
723 proteome (Bioassay 1). Cells were allowed to develop a full denitrification proteome under well-
724 fed conditions and were then washed twice in buffer prior to inoculation to flasks with YMB
725 (well-fed control) or buffer (starved), supplemented with 1 mM KNO_3 and 0.25 mM KNO_2, and
726 with He plus 1 ml N_2O (around 80 µmol N) in headspace. A larger inoculum was given to the
727 flasks with buffer (9.9E+08 cells flask^{-1}) than to the flasks with YMB (5.0E+09 cells flask^{-1}), to
728 secure measurable activity in the starved cells and adequate time resolution of the
729 denitrification kinetics in the well-fed cells. Panels A and B show the denitrification kinetics in
730 well-fed and starved cultures, respectively. The flasks were practically anoxic from the start with
731 an initial O_2 concentration in the liquid of <0.52 µM which decreased to approximately 0 µM
732 (insets in A & B). Panels C and D show the cell specific electron flow rate. $V_{e\ total\ den}$ designates
733 the total electron flow to the denitrification reductases and $V_{e\ total\ incl\ O2}$ the total electron flow,
734 including that to denitrification and to O_2. The electron flow rate to the individual reductases is
735 designated as V_{eNap}, V_{eNir}, V_{eNor} and V_{eNos}. V_{eNir} and V_{eNor} were practically identical and cannot be

736 distinguished from one another in the figure. Inserted panels show V_{eNap} throughout, including
737 negative values which are due to slight errors in determination of N_2 and N_2O (V_{eNap} was
738 calculated by N-mass balance). Bars in all graphs show standard deviation (n=3).

739

740 **FIG 3** Bioassay 1 with single nitrogen oxides**.** Experimental conditions as for Fig. 2, but the
741 starving cells (in buffer) were provided with either NO_3^-, NO_2^- or N_2O in individual flasks (n=3 for
742 each treatment). Panels A-C show the gas kinetics in flasks provided with 1 mM NO_3^- (A), 0.5
743 mM NO_2^- (B), or 70 µmol N_2O-N added to the headspace (C). Panel D shows the cell-specific
744 electron flow rate (V_e) measured in buffer supplemented with NO_3^-, NO_2^- or N_2O; the O_2
745 concentration (left y-axis); and V_e as percentage of the rates in well-fed cultures (right y-axis).
746 The number of cells inoculated into the incubation flasks at the start (0 h of incubation in anoxic
747 buffer) was 3.6E+09 for all treatments. Bars show standard deviation (n=3).

748

749 **FIG 4** Denitrification in starved cells after addition of TMPD as an external electron donor.
750 Preparation of the cultures followed Bioassay 1 (Fig. 1A), except that 100 µM TMPD and 10 mM
751 ascorbate were injected into the flasks with starving cells 15 min before the first gas sampling.
752 Each flask was inoculated with 5.28E+08 cells (n=4 replicate flasks). The initial O_2 concentration
753 was 0.35 µM and decreased to approximately 0 within 5 h (inset in A). Bars show standard
754 deviation (n=4). Panel A: kinetics of NO_2^-, NO, N_2O and N_2 (O_2 in inserted panel). Panel B:
755 Calculated cell specific electron flow rate (V_e, fmol cell^{-1} h^{-1}) to each of the reductases Nap, Nir,
756 Nor, and NosZ, and the total electron flow rate (V_{etotal}). The electron flow to Nir was practically
757 identical to the electron flow to Nor (miniscule amounts of NO), and the two are shown as a

758 single graph ($V_{eNir/Nor}$). Inset plots show V_{eNap} throughout, including negative values which are
759 due to slight errors in determination of N_2 and N_2O (V_{eNap} was calculated by N-mass balance).

760

761 **FIG 5** Bioassay 2: stochasticity of starvation response, response to input of organic C and
762 quantification of denitrification enzymes. Altogether fifteen flasks were prepared following
763 Bioassay 2 (see Fig. 1B). All flasks were anoxic (<0.5 µM at the start of the incubation) and
764 contained 50 ml buffer supplemented with 1 mM KNO_3 and with He plus 1 ml N_2O in the
765 headspace. The NO_2^- concentrations, measured during the first 5 hours after incubation in the
766 buffer, were approximately 0.59±0.20 µM (not shown). The cultures separated into two distinct
767 phenotypes: nine flasks had "slow" respiration (panel A) and 6 flasks had "fast" respiration
768 (panel B). The electron flow to the individual reductases (fmol e^- $cell^{-1}$ h^{-1}) for the flasks with
769 slow and fast respiration are shown in panels C and D, respectively. Cultures with "slow"
770 respiration rate had a total electron flow rate of maximum 0.27 e^- $cell^{-1}$ h^{-1} (C) and cultures with
771 "fast" respiration rate had a total electron flow rate of 1.0-1.8 fmol e- $cell^{-1}$ h^{-1} (D). The inset plot
772 in panel C shows the electron flow to the individual denitrification reductases after the carbon
773 addition. The cultures (entire flasks, 50 ml) were sampled for proteomics analyses at different
774 time points (panels E and F). At timepoints throughout, marked by dashed vertical lines in
775 panels A and B, three flasks were harvested for proteomics analysis (including 0 h). The six flasks
776 with "fast" respiration were harvested for proteomics analysis at 5 and 20 h of incubation in
777 these anoxic buffers (triplicates at each sampling point). Of the nine flasks with "slow"
778 respiration, three were harvested at 10 and three at 20 h. The remaining three "slow"
779 respiration flasks were supplemented with YMB at 24.8 h, at a concentration which made the

780 buffer a half-strength YMB medium, containing 5 g mannitol l^{-1} and 0.25 yeast extract l^{-1}, and
781 then harvested for proteomics at 27 h. The gas measurements and electron flows are averages
782 from the three flasks (n=3) for each phenotype, that were left untouched until the end of the
783 incubation when they were sampled for proteomics. Proteomics analyses were done for
784 triplicate flasks (n=3) at each sampling point. Standard deviations are indicated as bars in all
785 graphs (in several cases not visible due to low variation).
786

Bioassay 1: Denitrification induced before starvation

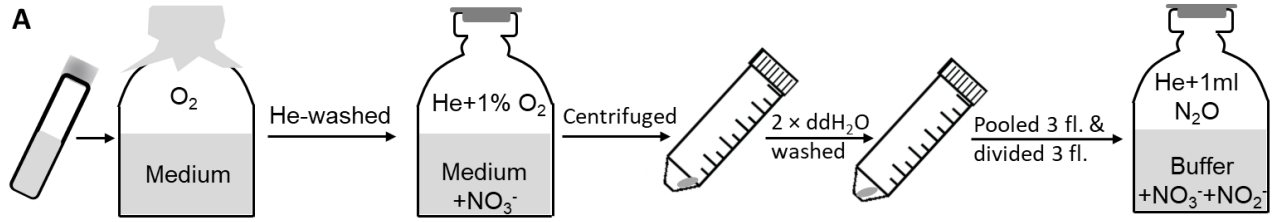

Bioassay 2: Denitrification induced during starvation

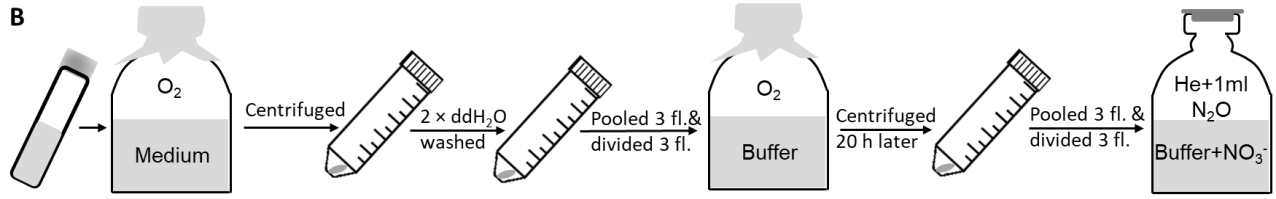

FIG 1 Bioassays for assessing the effect of starvation on electron flow to denitrification enzymes.
A: Bioassay 1: starvation of cells with a previously expressed denitrification proteome. Cells were raised from stock cultures in fully oxic flasks containing YMB medium. When OD_{600} reached ~0.1, the flasks were made anoxic by He-washing, then supplemented with 1% O_2 in the headspace and 1 mM NO_3^- in the liquid. The cultures were allowed to deplete the O_2 and to initiate denitrification when growing in YMB medium, after which they were centrifuged (10 000 × g at 4 °C for 10 mins) and washed twice in sterile ddH_2O. The pellets from triplicate flasks were pooled and used to inoculate flasks containing either C-free buffer or YMB medium (well-fed control), in both cases supplemented with 1 mM KNO_3 and 0.25 or 0.5 mM KNO_2, and with He and 1 ml N_2O (around 80 µmol N $flask^{-1}$) in headspace. The starving cells, incubated in buffer, had a low respiratory electron flow rate (mol electrons $cell^{-1}$ h^{-1}), initially being 10-18 % that of the well-fed cultures, and then decreasing to reach around 4% after 20 h. Results from experiments using Bioassay 1 are presented in Figs. 2, 3 and 4.
B: Bioassay 2: denitrification induced during starvation. Cells were raised from stock cultures in fully oxic flasks containing YMB medium. When OD_{600} reached ~0.1, the cultures were centrifuged (10 000 × g at 4 °C for 10 mins) and washed twice in sterile ddH_2O. The pellets from triplicate flasks were pooled, after which they were evenly divided and used to inoculate fully oxic flasks containing C-free buffer. These cultures were incubated for 20 h, then centrifuged after which the pellets were pooled and divided evenly before being inoculated into flasks containing C-free buffer-provided with 1 mM KNO_3, and with He and 1 ml N_2O (around 80 µmol N $flask^{-1}$) in headspace. The respiration rate (mol electrons $cell^{-1}$ h^{-1}) of the starving cultures was 1-4% compared to that of well-fed cultures. All cultures in Bioassays 1 and 2 were incubated at 28°C, and with vigorous stirring (650 rpm). Results from experiments using Bioassay 1 are presented in Figs. 5 and S2.

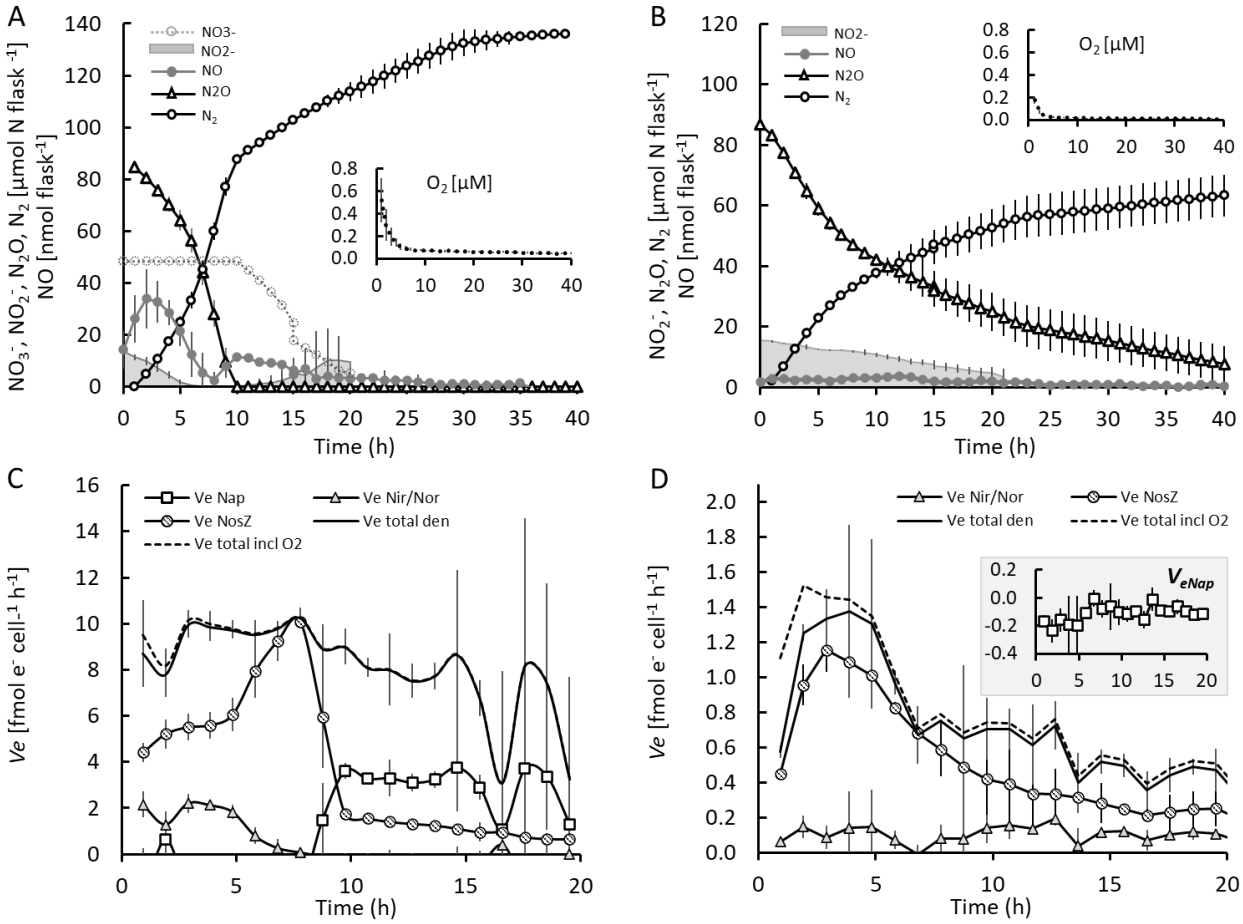

FIG 2 Denitrification kinetics as affected by starvation in cultures with a complete denitrification proteome (Bioassay 1). Cells were allowed to develop a full denitrification proteome under well-fed conditions and were then washed twice in buffer prior to inoculation to flasks with YMB (well-fed control) or buffer (starved), supplemented with 1 mM KNO_3 and 0.25 mM KNO_2, and with He plus 1 ml N_2O (around 80 µmol N) in headspace. A larger inoculum was given to the flasks with buffer (9.9E+08 cells flask^{-1}) than to the flasks with YMB (5.0E+09 cells flask^{-1}), to secure measurable activity in the starved cells and adequate time resolution of the denitrification kinetics in the well-fed cells. Panels A and B show the denitrification kinetics in well-fed and starved cultures, respectively. The flasks were practically anoxic from the start with an initial O_2 concentration in the liquid of <0.52 µM which decreased to approximately 0 µM (insets in A & B). Panels C and D show the cell specific electron flow rate. $V_{e\ total\ den}$ designates the total electron flow to the denitrification reductases and $V_{e\ total\ incl\ O2}$ the total electron flow, including that to denitrification and to O_2. The electron flow rate to the individual reductases is designated as V_{eNap}, V_{eNir}, V_{eNor} and V_{eNos}. V_{eNir} and V_{eNor} were practically identical and cannot be distinguished from one another in the figure. Inserted panels show V_{eNap} throughout, including negative values which are due to slight errors in determination of N_2 and N_2O (V_{eNap} was calculated by N-mass balance). Bars in all graphs show standard deviation (n=3).

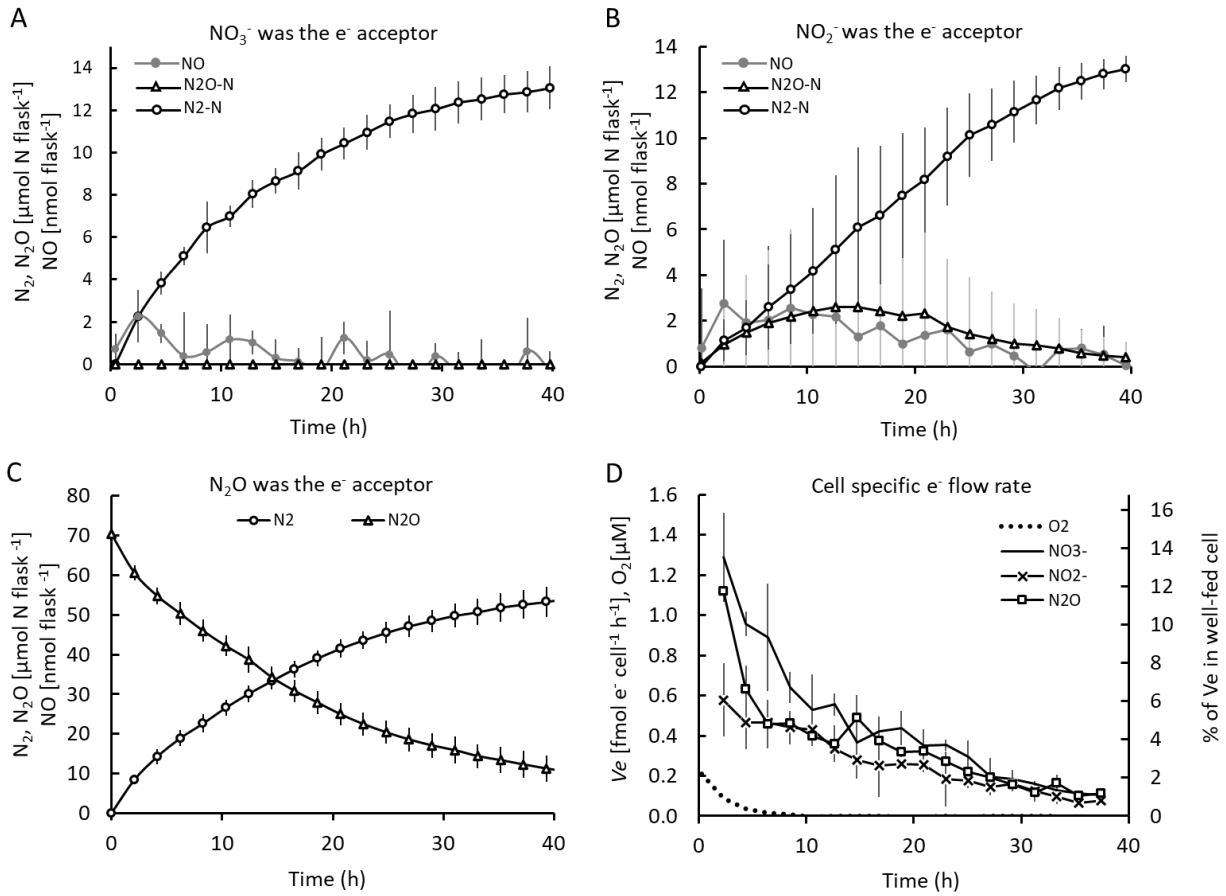

FIG 3 Bioassay 1 with single nitrogen oxides**.** Experimental conditions as for Fig. 2, but the starving cells (in buffer) were provided with either NO_3^-, NO_2^- or N_2O in individual flasks (n=3 for each treatment). Panels A-C show the gas kinetics in flasks provided with 1 mM NO_3^- (A), 0.5 mM NO_2^- (B), or 70 µmol N_2O-N added to the headspace (C). Panel D shows the cell-specific electron flow rate (V_e) measured in buffer supplemented with NO_3^-, NO_2^- or N_2O; the O_2 concentration (left y-axis); and V_e as percentage of the rates in well-fed cultures (right y-axis). The number of cells inoculated into the incubation flasks at the start (0 h of incubation in anoxic buffer) was 3.6E+09 for all treatments. Bars show standard deviation (n=3).

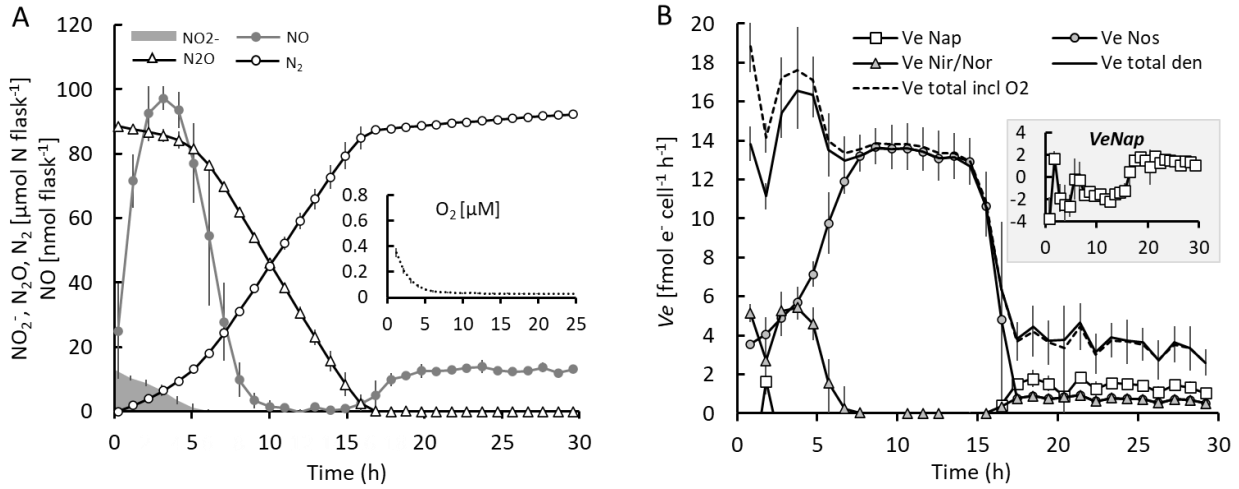

FIG 4 Denitrification in starved cells after addition of TMPD as an external electron donor. Preparation of the cultures followed Bioassay 1 (Fig. 1A), except that 100 µM TMPD and 10 mM ascorbate were injected into the flasks with starving cells 15 min before the first gas sampling. Each flask was inoculated with 5.28E+08 cells (n=4 replicate flasks). The initial O_2 concentration was 0.35 µM and decreased to approximately 0 within 5 h (inset in A). Bars show standard deviation (n=4). Panel A: kinetics of NO_2^-, NO, N_2O and N_2 (O_2 in inserted panel). Panel B: Calculated cell specific electron flow rate (V_e, fmol cell^{-1} h^{-1}) to each of the reductases Nap, Nir, Nor, and NosZ, and the total electron flow rate (V_{etotal}). The electron flow to Nir was practically identical to the electron flow to Nor (miniscule amounts of NO), and the two are shown as a single graph ($V_{eNir/Nor}$). Inset plots show V_{eNap} throughout, including negative values which are due to slight errors in determination of N_2 and N_2O (V_{eNap} was calculated by N-mass balance).

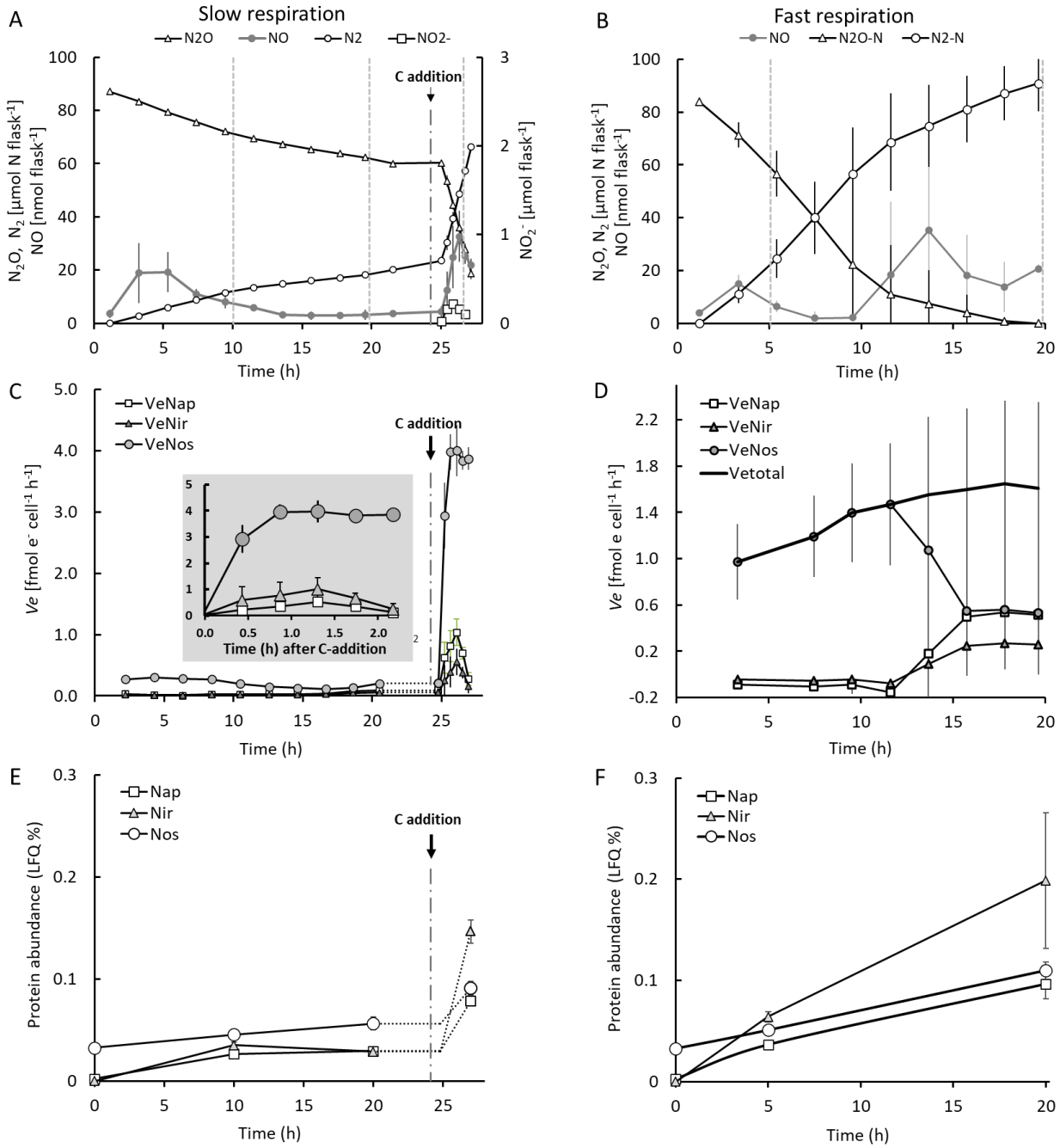

FIG 5 Bioassay 2: stochasticity of starvation response, response to input of organic C and quantification of denitrification enzymes. Altogether fifteen flasks were prepared following Bioassay 2 (see Fig. 1B). All flasks were anoxic (<0.5 µM at the start of the incubation) and contained 50 ml buffer supplemented with 1 mM KNO_3 and with He plus 1 ml N_2O in the headspace. The NO_2^- concentrations, measured during the first 5 hours after incubation in the buffer, were approximately 0.59±0.20 µM (not shown). The cultures separated into two distinct phenotypes: nine flasks had "slow" respiration (panel A) and 6 flasks had "fast" respiration (panel B). The electron flow to the individual reductases (fmol e^- $cell^{-1}$ h^{-1}) for the flasks with slow and fast respiration are shown in panels C and D, respectively. Cultures with "slow" respiration rate had a total electron flow rate of maximum 0.27 e^- $cell^{-1}$ h^{-1} (C) and cultures with "fast" respiration rate had

a total electron flow rate of 1.0-1.8 fmol e- $cell^{-1}$ h^{-1} (D). The inset plot in panel C shows the electron flow to the individual denitrification reductases after the carbon addition. The cultures (entire flasks, 50 ml) were sampled for proteomics analyses at different time points (panels E and F). At timepoints throughout, marked by dashed vertical lines in panels A and B, three flasks were harvested for proteomics analysis (including 0 h). The six flasks with "fast" respiration were harvested for proteomics analysis at 5 and 20 h of incubation in these anoxic buffers (triplicates at each sampling point). Of the nine flasks with "slow" respiration, three were harvested at 10 and three at 20 h. The remaining three "slow" respiration flasks were supplemented with YMB at 24.8 h, at a concentration which made the buffer a half-strength YMB medium, containing 5 g mannitol l^{-1} and 0.25 yeast extract l^{-1}, and then harvested for proteomics at 27 h. The gas measurements and electron flows are averages from the three flasks (n=3) for each phenotype, that were left untouched until the end of the incubation when they were sampled for proteomics. Proteomics analyses were done for triplicate flasks (n=3) at each sampling point. Standard deviations are indicated as bars in all graphs (in several cases not visible due to low variation).